JOURNAL OF CATALYSIS **127**, 267–275 (1991)

# The Hydrogenation of Toluene and *o*-, *m*-, and *p*-Xylene over Palladium

## II. Reaction Model

M. VASIUR RAHAMAN AND M. ALBERT VANNICE

*Department of Chemical Engineering, Pennsylvania State University, University Park, Pennsylvania 16802*

Received April 3, 1990; revised September 10, 1990

The similarity among activation energies and partial pressure dependencies for the hydrogenation of benzene, toluene, and the three xylene isomers allowed the use of our previous model for benzene hydrogenation, which could be simplified for the hydrogenation of toluene and the xylenes because there was no evidence of deactivation or significant coverages of hydrogen-deficient surface inhibitors. Thus a Langmuir–Hinshelwood model involving two sets of active sites, one on the Pd surface and the other composed of acid sites in the Pd-support interfacial region supplied by spilled-over hydrogen, readily describes the kinetics for these four aromatic hydrocarbons as well as benzene. The presence of these acid sites, presumed to be Brønsted sites, was confirmed by the parallel reaction of *o*-xylene isomerization to *m*-xylene, and rate enhancements in this reaction were nearly identical to those observed for the hydrogenation of *o*-xylene. The derived rate expression was computer fitted to the data and the obtained values of the equilibrium adsorption constants for $H_2$ and these aromatic compounds are consistent with assumptions in the model and provide trends in agreement with results from the literature.

## INTRODUCTION

The role of the support in catalytic reactions occurring in dispersed metal systems has been under close scrutiny during the past decade (*1*). Tenfold increases in specific activity have been obtained for benzene hydrogenation over Pd by the use of supports like $SiO_2$–$Al_2O_3$, zeolites, and $TiO_2$ (*2–4*); however, this effect is distinctly different from the metal-support interaction (sometimes designated SMSI) that enhances hydrogenation rates of CO and other carbonyl bonds over noble metals dispersed on $TiO_2$ (*5–9*). One notable difference is that a high-temperature reduction on $Pd/TiO_2$ (or $Pd/SiO_2$–$Al_2O_3$) eliminates this activity enhancement, whereas higher specific activities are obtained for CO hydrogenation on $Pd/TiO_2$ or $Pt/TiO_2$.

To explain this behavior, we recently proposed a model for benzene hydrogenation which invokes a contribution to the overall rate from active sites in the metal-support interfacial region (*10*). These are assumed to be acid sites on the oxide surface which adsorb these basic aromatic hydrocarbons and are supplied by hydrogen migrating short distances from the Pd particle surfaces. Thus the concentration of these sites, particularly Brønsted acid sites, can have a significant effect on the overall activity.

In the first paper in this series, the hydrogenation of toluene and *o*-, *m*-, and *p*-xylene was examined in detail, and kinetic parameters were obtained and compared to those for benzene (*11*). The similarities indicated that our previous model was applicable and, in fact, could be simplified. This is discussed here in greater detail. In addition, an important aspect of this current study was the observation that *o*-xylene isomerization to *m*-xylene, a reaction that occurs on acidic sites via a carbonium mechanism (*12*), occurred simultaneously with hydrogenation. Thus an internal probe was available that was sen-

0021-9517/91 $3.00

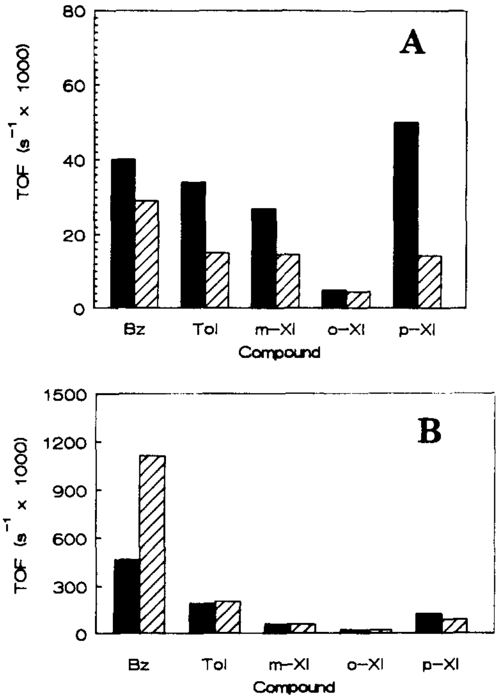

FIG. 1. Turnover frequencies for the hydrogenation of aromatic hydrocarbons at 413 K, 50 Torr aromatic compound, and 680 Torr hydrogen: Benzene, Bz; toluene, Tol; *m*-xylene, *m*-Xl; *o*-xylene, *o*-Xl; *p*-xylene, *p*-Xl (from Ref. (*11*)). (A) Pd powder, solid bars; Pd/MgO, striped bars. (B) Pd/$SiO_2$–$Al_2O_3$ (448 K), striped bars; Pd/$TiO_2$ (448 K), solid bars.

sitive to the support acidity, and quantification of the reaction rates for isomerization provided additional justification for our proposed model.

## RESULTS AND DISCUSSION

The kinetic results and rate data utilized here are reported in the preceding paper (*11*). An example of relative reaction rates for the hydrogenation of benzene, toluene, and the three xylene isomers in the absence of acidic supports is shown in Fig. 1A. Large differences in turnover frequency (TOF) do not exist although *o*-xylene always has the lowest activity. This behavior can be compared to that for Pd dispersed on the most acidic supports, shown in Fig. 1B. The TOFs are higher in all reactions, as indicated by the larger ordinate scale, and the activity pattern is similar, but in contrast the rates for benzene and toluene hydrogenation are much more significantly enhanced when acidic supports are used.

During *o*-xylene hydrogenation, isomerization to *m*-xylene also occurred. The isomerization of *o*- to *m*-xylene by acid-catalyzed carbonium ion chemistry is well known, and this reaction has been used to estimate the concentration of acid sites on acidic oxides (*13*). Investigations have shown that benzene and toluene adsorb on acidic oxide surfaces (*14–19*), and the formation of carbonium ions by the interaction of toluene with Brønsted acid sites on $TiO_2$ and H-ZSM-5 has been observed (*15, 16*) Adsorption via the $\pi$-electrons of the aromatic molecule is presumed to occur, with the extent of irreversible adsorption on $TiO_2$ increasing with increasing $\pi$-electron concentration (*17, 18*). Thus these aromatic molecules are anticipated to adsorb on surface acid sites, with carbonium ions most likely forming after proton transfer from Brønsted sites, which are known to exist on both $SiO_2$–$Al_2O_3$ and $TiO_2$ (*13, 20*). Halogens can polarize surface hydroxyl groups and increase the acidity of these sites (*21*). Although titania is amphoteric, impurities can produce strong acid sites (*20*), and HCl generated during the reduction step of the $PdCl_4^{2-}$ anion can create acid sites (*22*). Furthermore, chlorine can be removed during high-temperature treatments, and surface chloride begins to be removed by reduction in $H_2$ at 473 K (*23*). The used samples of either Pd/$TiO_2$ or Pd/$SiO_2$–$Al_2O_3$ had a higher $Cl^-$ content after reduction at 448 K than after 673 K (*24*), in agreement with the literature.

The rates of *o*-xylene isomerization given in Table 7 of the preceding study (*11*) clearly establish the presence of acid sites in some of these systems, particularly when $TiO_2$ and $SiO_2$–$Al_2O_3$ are used after a low-temperature reduction, and they are consistent with the supposition that Brønsted sites are primarily involved in catalytic activity, as suggested earlier (*10*) and as shown by *m*-xylene isomerization over zeolite catalysts (*25*). The isomerization turnover frequency on Pd in the absence of any contribution from acid sites on the support can be obtained from the Pd powder, Pd/MgO, and Pd/$SiO_2$ catalysts, which give an average TOF of 0.0049 ± 0.0005 $s^{-1}$ under our reaction conditions. Reduction at 673 K converts Brønsted acid sites into Lewis acid sites on $Al_2O_3$ (*26*), and indeed only a very small contribution, if any, is indicated for the Pd/$Al_2O_3$ catalyst. As depicted in Table 2, the most acidic supports give a fivefold increase in the specific activity for isomerization and, as expected for $TiO_2$ (*23*), reduction at 673 K removes both Cl and Brønsted acid sites thus reducing activity. The higher-temperature reduction also decreases the rate contribution from the $SiO_2$–$Al_2O_3$ support. The lower activity of the acidic oxides in the absence of Pd compared to these same oxides with Pd is likely due to the absence of activated hydrogen migration off the Pd, which can keep the acid sites cleaned of carbonaceous residues (*27*). Regardless, the highest concentrations of these sites on the most active hydrogenation catalysts is clearly established.

There is much similarity between the hydrogenation reaction model proposed here and that for benzene hydrogenation proposed earlier by Chou and Vannice (*10*); in fact, the one here is simpler because no deactivation of the catalysts was observed during the hydrogenation of toluene or the three xylenes. Orozco and Webb had previously reported no toluene retention on either Pd/$SiO_2$ or Pd/$Al_2O_3$ (*28*). This suggests that little, if any, dehydrogenation occurs to form carbonaceous residues, hence surface coverage by any carbonaceous residue is assumed to be negligible. This trend is consistent with the greater stability of the $\pi$-bonds in these aromatics compared to benzene. It was found that the TOF is dependent on both the support and the reduction temperature of the catalysts with acidic supports (*11*). The explanation advanced for the higher TOFs with the acidic supports is that additional active sites can exist in the metal-support interface region which can also participate in the hydrogenation of aromatic hydrocarbons. All five reactions, including benzene, are first order in $H_2$ and zero order in hydrocarbon concentration under these reaction conditions (*4*, *11*), thus indicating near-saturation coverage of the active sites by aromatic species. A higher heat of adsorption for the aromatic compound favors its preferential adsorption over $H_2$, especially since $H_2$ needs two sites to dissociate. As toluene and the three xylenes are expected to have stronger interactions with Pd than benzene (*29–31*), the first-order dependence on benzene is expected to be retained.

The enhancement in specific activity can be very pronounced, as shown in Fig. 1, which compares the TOFs on Pd powder and Pd dispersed on the basic MgO support with the TOF values for the two most acidic catalysts. Except for *o*-xylene, hydrogenation rates do not vary markedly in the absence of an acidic support, whereas the use of an acidic support and a low-temperature reduction near 448 K enhances all rates, with those for benzene and toluene being increased the most.

Using arguments and assumptions similar to those made previously (*10*), the latter of which are itemized in Table 1, the reaction model proposed is depicted in Fig. 2 using toluene as an example. Weakly bound, highly mobile hydrogen has been shown to exist on the Pd surface (*32*, *33*), and van Meerten *et al.* have shown it to be dissociatively adsorbed (*34*). This weakly chemisorbed hydrogen appears to constitute the species reacting with aromatic compounds (*34–36*). Neither the adsorption of the aromatic hydrocarbon nor the desorption of the paraffinic product should be a rate-determining step (rds) (*37*). Thus one of the stepwise additions of hydrogen atoms to the adsorbed aromatic molecule is anticipated to be the rds, should one exist, as shown for benzene (*38*, *39*).

For a given reaction, activation energies

TABLE 1

Assumptions for the Reaction Model

1. Adsorption of the aromatic compound occurs on both Pd and the support surfaces.
2. Adsorption of hydrogen on the Pd surface provides activated hydrogen, which can migrate to the interfacial region via spillover.
3. Quasi-equilibrium exists between the hydrogen on Pd and spilled-over hydrogen in the interface region.
4. Hydrogen and the hydrocarbons adsorb on different types of sites.
5. The reaction occurs simultaneously on both Pd crystallites and acid sites in the interface region (see Fig. 2).
6. The adsorbed aromatic reactant species is the most abundant surface intermediate; i.e., surface coverage of all other reaction intermediates is negligible. Furthermore, near saturation exists at higher pressures so that $K_AP_A \gg 1$ and a zero-order dependence exists.
7. The reactive hydrogen species is more weakly bound; thus the coverages are relatively low, ($K_{H_2}P_{H_2} \ll 1$) and a first-order dependence occurs.
8. The rate-determining step (rds) is the addition of the second H atom (or the simultaneous addition of the first two atoms, possibly by an activated $H_2$ molecule).
9. Desorption of the product from both regions occurs easily.

and pressure dependencies appear to be independent of the support (*4, 11*); therefore, the sequence of elementary steps that follows is assumed to be the same for all four aromatic compounds on Pd:

$$H_2(g) + 2S \overset{K_{H_2}}{\longleftrightarrow} 2H\text{-}S \qquad (1)$$

$$A(g) + * \overset{K_A}{\longleftrightarrow} A\text{-}* \qquad (2)$$

$$A\text{-}* + H\text{-}S \overset{K_1}{\longleftrightarrow} A_1\text{-}* + S \qquad (3)$$

$$A_1\text{-}* + H\text{-}S \xrightarrow[\text{rds}]{k} A_2\text{-}* + S \qquad (4)$$

$$A_2\text{-}* + H\text{-}S \overset{K_3}{\longleftrightarrow} A_3\text{-}* + S \qquad (5)$$

$$\cdots \qquad (6)$$

$$\cdots \qquad (7)$$

$$A_5\text{-}* + H\text{-}S \overset{K_6}{\longleftrightarrow} P\text{-}* + S \qquad (8)$$

$$P\text{-}* \overset{1/K_P}{\longleftrightarrow} P(g) + *, \qquad (9)$$

where $S$ is an adsorption site for H, $A$ is the aromatic reactant molecule, * is an adsorption site for $A$, $A_i$ is an intermediate obtained after adding $i$ number of hydrogen atoms, and $P$ is the cycloparaffin product. This gives a rate expression of the form

$$r_{Pd} = k_{Pd}K_1 \left(\frac{K_{H_2}P_{H_2}}{1 + \sqrt{K_{H_2}P_{H_2}}}\right)\left(\frac{K_AP_A}{1 + K_AP_A}\right) \qquad (10)$$

Assumption 3 in Table 1 produces an identical form of the final rate expression for the active sites on the oxide support if a separate site for spilled-over hydrogen is defined (*24*). Alternatively, if just a migrating hydrogen atom is assumed to exist, a first-order dependence on $H_2$ is obtained and the rate expression for these interfacial sites is

$$r_I = k_IK_I'K_{H_2}P_{H_2}\left(\frac{K_A'P_A}{1 + K_A'P_A}\right) \qquad (11)$$

This is identical to the former expression for small $K_{H2}$ values, i.e., at low hydrogen coverages. NMR studies of weakly adsorbed hydrogen on Pd have shown that it exchanges readily with hydroxyl groups on silica (*33*), thus providing support for this postulate. The total rate is the sum of that

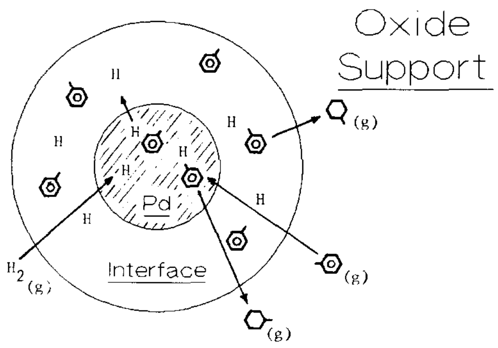

FIG. 2. Reaction model invoking interfacial sites for the hydrogenation of aromatic hydrocarbons over Pd dispersed on acidic oxide supports.

on the Pd and that on the interface sites; i.e., $r_T = r_{Pd} + r_I$ or $TOF_T = TOF_{Pd} + TOF_I$ because total rates are normalized to the Pd surface area. Employing a Langmuir–Hinshelwood model along with the assumptions in Table 1 and the experimental result that all reaction orders on $H_2$ were near first order, the final rate expression for catalysts with an acidic support simplifies to

$$TOF_T = k_{Pd}K_1K_{H_2}P_{H_2}\left(\frac{K_AP_A}{1 + K_AP_A}\right) + k_IK'_IK_{H_2}P_{H_2}\left(\frac{K'_AP_A}{1 + K'_AP_A}\right) \quad (12)$$

At high enough pressures of the aromatic compound this just becomes

$$TOF_T = (k'_{Pd} + k'_I)P_{H_2} \quad (13)$$

Assumption 6 in Table 1 is substantiated by the fact that cyclohexadienes and cyclohexenes hydrogenate much more rapidly than the original aromatic reactant (*40*). TOF values can be orders of magnitude higher, as shown by Gonzo and Boudart who measured a value of 5.3 $s^{-1}$ at 288 K for cyclohexene over Pd (*41*). At our reaction conditions at 413 K, the extrapolated TOF value of 970 $s^{-1}$ is $10^3$–$10^4$ times higher than that for benzene (*4*).

Based on Eq. (11), the average hydrogenation rate on Pd alone can be determined from that measured for Pd powder, Pd/MgO, $Pd/SiO_2$, and $Pd/Al_2O_3$ and, because all these reactions appear to be structure insensitive (*11*), this contribution can be subtracted from the total rate to obtain the relative enhancement from the acidic support. These values are given in Table 2, and they reveal that the greatest contribution from the support sites is during benzene hydrogenation and it declines as methyl groups are added to the benzene ring. A complete explanation for this is not available at this time, but the trend does correlate with the ionization potential of the aromatic molecule. The presence of acidic sites on the support is verified by the enhanced isomerization activity when the acidic supports are used, and it is noteworthy that the rate increase for isomerization over these two catalysts is almost equal to the rate increase in hydrogenation (3.9 vs 4.4).

TABLE 2

Contribution of Interfacial Acid Sites to Hydrogenation of Aromatic Hydrocarbons Relative to Sites on Pd

| Hydrocarbon | $r_I/r_{Pd}$[a] | |
|---|---|---|
| | $Pd/SiO_2$–$Al_2O_3$ | $Pd/TiO_2$ |
| Benzene | 27.0 | 12.0 |
| Toluene | 6.8 | 6.4 |
| *o*-Xylene | 4.4 | 4.4 |
| *m*-Xylene | 2.3 | 2.3 |
| *p*-Xylene | 2.6 | 4.1 |
| *o*-Xylene[b] | 3.9 | 3.9 |

[a] $r_I/r_{Pd} = (TOF_T - TOF_{Pd})/TOF_{Pd}$, where $TOF_{Pd}$ is the average on Pd powder, Pd/MgO, $Pd/SiO_2$, and $Pd/Al_2O_3$ at 413 K, 680 Torr $H_2$ and 50 Torr aromatic.

[b] For isomerization reaction.

The proposed sequence of elementary steps is quite reasonable as the initial destabilization of the resonance structure would be anticipated to be the most difficult step. This would not only explain the invariance in activation energy for a given reaction over unsupported Pd and Pd dispersed on both acidic and nonacidic supports, but also would account for the small increase observed with increasing resonance energy of the aromatic ring. However, an alternative sequence providing the same final rate expression would involve the addition of two H atoms simultaneously or the addition of an activated $H_2$ molecule, thus combining steps (3) and (4) into a single rds. The latter may be somewhat preferable as it involves only a two-body interaction. Di-$\sigma$-bonded benzene species have been reported by Gland and Somorjai (*42*), which would conveniently fit the suggested sequence of steps; however, such species would not be anticipated on Brønsted acid sites. In addition, based only on steric considerations and

TABLE 3

Regressed Values for Parameters in the Rate Expression for Hydrogenation of Toluene, *o*-Xylene, and *m*-Xylene over Pd/$Al_2O_3$[a]

| Compound | $T_{rxn}$ (K) | $k_{Pd}$ ($s^{-1}$) | $E$ $\left[\frac{kcal}{mol}\right]$ | $A^b$ ($s^{-1} \times 10^{-7}$) | $K_{H_2}$ ($atm^{-1} \times 10^3$) | $K_A$ ($atm^{-1}$) |
|---|---|---|---|---|---|---|
| Benzene[c] | 363 | 2.4 | 12.4 | 7.4 | 5.6 | 227 |
| Toluene | 413 | 23.1 | 11.8 | 31 | 3.0 | 130 |
| *m*-Xylene | 438 | 19.5 | 14.2 | 25 | 2.3 | 419 |
| *o*-Xylene | 438 | 5.2 | 14.9 | 15 | 2.0 | 1160 |

[a] $TOF_{Pd} = k_{Pd}[K_AP_A/(1 + K_AP_A)][K_{H_2}P_{H_2}/(1 + \sqrt{K_{H_2}P_{H_2}})^2]$.
[b] $k_{Pd} = Ae^{-E/RT}$.
[c] From Ref. (*10*).

probability arguments, adsorbed di-$\sigma$-bonded *o*-xylene should be favored over the other two isomers by a $\frac{3}{2}$ ratio. As the lowest rates occur with *o*-xylene, our results do not support this species as an intermediate.

The activation energies and partial pressure dependencies for each reaction over the various catalysts were very similar, hence Pd/$Al_2O_3$ was chosen to represent the low activity, nonacidic group and Pd/$SiO_2$–$Al_2O_3$ (448 K) was chosen to represent the high activity, acidic group of catalysts. The partial pressure data for Pd/$Al_2O_3$ from Ref. (*24*) were fitted to Eq. (10) using the activation energies from Ref. (*11*). The data were nonlinearly regressed by a Narquardt algorithm utilizing a NLIN procedure available in an SAS package on an IBM mainframe computer at this university. A problem with using a data-fitting procedure such as this is that the parameters may not converge to unique values, and final values may depend on the initial guesses. However, no a priori constraints were imposed to obtain the optimized parameter values, and a wide variety of initial guesses typically yielded final parameter values which agreed to within ±5%. These values for $K_{Pd}$, $K_{H_2}$, and $K_A$ are listed in Table 3, and the best fits obtained with these parameters for toluene, *o*-xylene, and *m*-xylene hydrogenation over Pd/$Al_2O_3$ are shown in Figs. 3, 4, and 5, respectively.

To estimate the kinetic parameters for the interfacial sites, the appropriate activation energy was used to adjust the rates measured during the reaction order study to 413 K; that is, toluene rates were raised from 363 K and *o*- and *m*-xylene rates were lowered from 438 K. Then, based on the Pd/$Al_2O_3$ catalyst and using Eq. (12), the contribution from the Pd surface was subtracted from the total rate and the difference was fitted by Eq. (11). The total rate of the Pd/$SiO_2$–$Al_2O_3$ catalyst could also be fit easily by an equation of the form of Eq. (11), which

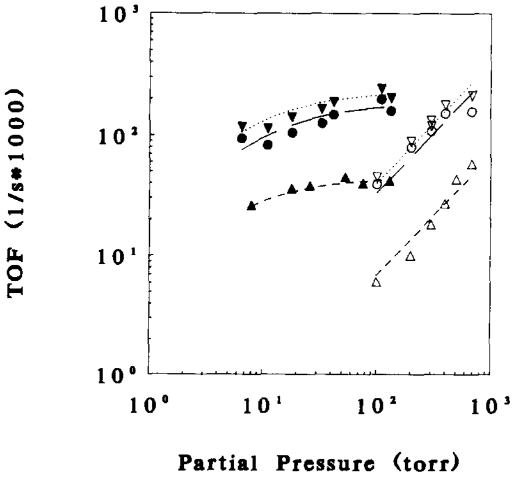

FIG. 3. Rate dependencies on toluene (solid symbols) and $H_2$ (open symbols) at 413 K over 1.1% Pd/$SiO_2$–$Al_2O_3$ (▼, ▽) and 1.5% Pd/$Al_2O_3$ (▲, △). Rate dependency for interfacial sites by difference (●, ○); lines represent fitting by model.

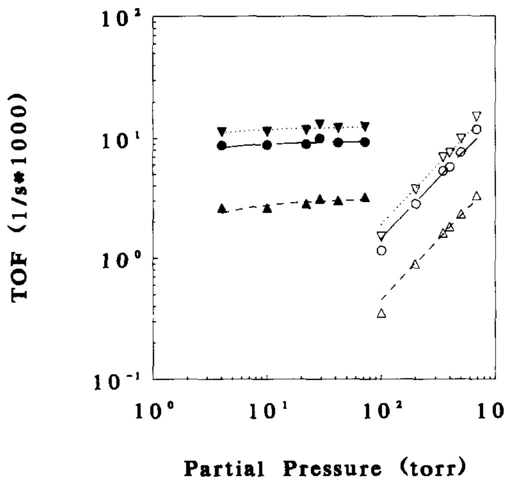

FIG. 4. Rate dependencies on *o*-xylene (solid symbols) and $H_2$ (open symbols) at 413 K over 1.1% Pd/$SiO_2$–$Al_2O_3$ (▼, ▽) and 0.5% Pd/$Al_2O_3$ (▲, △). Rate dependency for interfacial sites by difference (●, ○); lines represent fitting by model.

TABLE 4

Regressed Values for Parameters in the Rate Expression for Toluene, *o*-Xylene, and *m*-Xylene Hydrogenation over Pd Catalysts at 413 K

| Catalyst | Aromatic | $k$ ($s^{-1}$) | $k'$ ($s^{-1} \cdot atm^{-1}$)[a] | $K_A$ ($atm^{-1}$) |
|---|---|---|---|---|
| 1.1% Pd/$SiO_2 \cdot Al_2O_3$ | Toluene | 0.230[b] | 0.291 | 100 |
| | *m*-Xylene | 0.055[b] | 0.070 | 600 |
| | *o*-Xylene | 0.013[b] | 0.016 | 1600 |
| Pd/$Al_2O_3$ | | | | |
| 1.5% Pd | Toluene | 0.045[c] | 0.057 | 130 |
| 0.5% Pd | *m*-Xylene | 0.014[c] | 0.017 | 500 |
| 0.5% Pd | *o*-Xylene | 0.0031[c] | 0.0039 | 600 |
| $\Delta r = r_I$ | Toluene | 0.185[d] | 0.235 | 80 |
| | *m*-Xylene | 0.042[d] | 0.053 | 600 |
| | *o*-Xylene | 0.0094[d] | 0.012 | 1500 |

[a] $k' = k/P_{H_2}$.
[b] $k = k_T K_1'' K_{H_2} P_{H_2}$, i.e., $TOF = kK_A P_A/(1 + K_A P_A)$.
[c] $k = k_{Pd} K_1 K_{H_2} P_{H_2}$ from Eq. (10).
[d] $k = k_I K_1' K_{H_2} P_{H_2}$ from Eq. (11).

is not surprising because the dominant contribution was from the interfacial sites. These results and the fits provided by the model are also shown in Figs. 3–5, and the rate parameters corresponding to these predicted rates are listed in Table 4. The constraint of a first-order dependence on $H_2$ did not have a large effect on the parameters for Pd/$Al_2O_3$ in Table 4 except for *o*-xylene, which had a $K_A$ value only half that in Table 3. The *k* values typically converged within a small uncertainty limit (±10%) independently of the initial guess; however, a greater variation existed among the $K_A$ values and those in Table 4 represent average values.

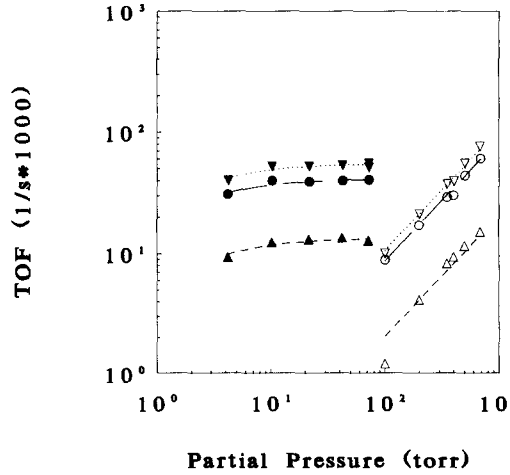

FIG. 5. Rate dependencies on *m*-xylene (solid symbols) and $H_2$ (open symbols) at 413 K over 1.1% Pd/$SiO_2$–$Al_2O_3$ (▼, ▽) and 0.5% Pd/$Al_2O_3$ (▲, △). Rate dependency for interfacial sites by difference (●, ○); lines represent fitting by model.

It must be kept in mind that the $K_A$ and $K_{H_2}$ values in Table 3 are associated only with the Pd surface for the nonacidic Pd/$Al_2O_3$ catalysts, whereas the contribution from the support dominates in the Pd/$SiO_2$–$Al_2O_3$ sample, thus the values can be associated primarily with the acid sites in the latter sample. In support of assumptions 2 and 3 in Table 1, these values indicate that the equilibrium adsorption constants, $K_A$, for these three aromatic compounds are much larger than unity and those for $K_{H_2}$ are much less than unity. Furthermore, the $K_A$ values tend to increase with increasing basicity of the reactant molecule, whereas the $K_{H_2}$ values are similar on the nonacidic Pd/$Al_2O_3$ catalyst in the presence of the three different aromatic adsorbates. Finally, preexponential values varied by only a factor of four on the nonacidic catalyst, again indicating a similarity in the surface chemistry associated with the four reactants. The computer fitting with Eq. (12) to give the lumped parameters in Table 4 does not provide as much information; however, the $K_A$ values for $Pd/Al_2O_3$ not only exhibit the same trend as in Table 3 but the absolute values are also similar. As expected, the reaction orders for the rate associated with the interfacial sites ($TOF_I$ or $r_I$) are first order in $H_2$ and near zero order in the aromatic compound, as indicated in Figs. 3–5. However, the $K'_A$ values associated with the acid sites on the support vary over a much wider range than those associated with the Pd surface, and they imply that the model is sensitive to differences between the two types of sites.

Finally, it is worthwhile comparing the ratio of equilibrium adsorption constants for benzene and toluene in Table 3 to that reported by Phoung *et al.* (*30*). Our $K_T/K_B$ ratio of 0.6 is very close to the value of 1.0 they reported for the competitive hydrogenation of mixtures of these two hydrocarbons over a $Pd/SiO_2$ catalyst (*30*). This is remarkably good agreement and provides confidence in the reaction model proposed here and the consistency of our data-fitting procedure.

## SUMMARY

A Langmuir–Hinshelwood model assuming that hydrogen and the aromatic hydrocarbon adsorb on different sites readily describes the hydrogenation of benzene, toluene, and *o*-, *m*-, and *p*-xylene on Pd dispersed on both acidic and nonacidic supports. An additional proposal is that acid sites in the interfacial region around the Pd crystallites can adsorb these basic hydrocarbons, which are subsequently hydrogenated by spilled-over hydrogen. Thus the higher activities obtained with acidic supports are attributed to this additional reaction because the Pd surface is near saturation with the aromatic hydrocarbon, and the presence of these active centers, presumably Brønsted acid sites, was confirmed by the enhanced activity of the *o*- to *m*-xylene isomerization reaction when acidic supports were used. This occurred simultaneously with the hydrogenation reaction and specific activities on both the Pd and the oxide surfaces were measured.

Computer-fitting the derived rate equation to the data provided values for the preexponential factors and equilibrium adsorption constants for $H_2$ and the aromatic hydrocarbons over the nonacidic $Pd/Al_2O_3$ catalyst. For the acidic $Pd/SiO_2-Al_2O_3$ sample, only equilibrium adsorption constants for toluene, *o*-xylene, and *m*-xylene could be obtained. These values are reasonable and are consistent with assumptions in the model as well as with expectations from the literature. In addition, variations in their values imply significant differences between the sites on Pd compared to those that predominate when acidic supports are used.

## ACKNOWLEDGMENTS

This study was supported by the U.S. Department of Energy, Division of Basic Energy Sciences, under Grant DE-FG02-84ER 13276. We also thank S. Lin for his assistance in some of the computer-fitting efforts.

## REFERENCES

*1.* Haller, G. L., and Resasco, D. E., *Adv. Catal.* **36,** 173 (1989).
*2.* Figueras, F., Gomez, R. and Primet, M., *Adv. Chem. Ser.* **121,** 480 (1973).
*3.* Vannice, M. A., and Chou, P., *Int. Congr. Catal. Proc. 6th 1984* **5,** 99 (1984).
*4.* Chou, P., and Vannice, M. A., *J. Catal.* **107,** 129 (1987).
*5.* Vannice, M. A., *J. Catal.* **74,** 199 (1982).
*6.* Wang, S. Y., Moon, S. H., and Vannice, M. A., *J. Catal.* **71,** 167 (1981).
*7.* Vannice, M. A., and Twu, C. C., *J. Catal.* **82,** 213 (1983).
*8.* Sen, B., and Vannice, M. A., *J. Catal.* **113,** 52 (1988).
*9.* Vannice, M. A., and Sen, B., *J. Catal.* **115,** 65 (1989).
*10.* Chou, P., and Vannice, M. A., *J. Catal.* **107,** 140 (1987).
*11.* Rahaman, M. V., and Vannice, M. A., *J. Catal.* **127,** 251 (1991).
*12.* Pines, H., "The Chemistry Of Catalytic Hydrocarbon Conversions," p. 24. Academic Press, New York, 1981.

13. Benesi, H. A., and Winquist, B. H. C., *Adv. Catal.* **27,** 97 (1978).
14. Peri, J. B., *J. Phys. Chem.* **70,** 3168 (1966).
15. Farneth, W. E., Roe, D. C., Gricus Kofke, T. J., Tabak, C. J., and Gorte, R. J., *Langmuir* **4,** 152 (1988).
16. Davydov, A. A., *Mater. Chem. Phys.* **19,** 97 (1988).
17. Suda, Y., *Langmuir* **4,** 147 (1988).
18. Nagao, M., and Suda, Y., *Langmuir* **5,** 42 (1989).
19. Eltekova, N., and Eltekov, Y., *Langmuir* **3,** 951 (1987).
20. Busca, G., Saussey, H., Saur, O., Lavelleu, J. C., and Lorenzelli, V., *Appl. Catal.* **14,** 245 (1985).
21. Chapman, I. D., and Hair, M. L., *Int. Congr. Catal. Proc. 3rd 1964* **2,** 1091 (1964).
22. Siriwardane, R. V., and Wightman, J. P., *J. Colloid Interface Sci.* **94,** 502 (1983).
23. Tiep, L. V., Bureau-Tardy, M., Bugli, G., Djega-Mariadassou, G., Che, M., and Bond, G. C., *J. Catal.* **99,** 449 (1986).
24. Rahaman, M. V., M.S. thesis, Pennsylvania State University, 1989.
25. Haag, W. O., and Chen, N. Y., *in* "Catalyst Design, Progress and Perspectives," Chap. 6. Wiley, New York, 1987.
26. Marczewski, M., Derewinski, M., and Malinowski, S., *Canad. J. Chem. Eng.* **61,** 93 (1983).
27. Gates, B. C., Katzer, J. R., and Schuit, G. C. A., *in* "Chemistry of Catalytic Processes," Chap. 3. McGraw–Hill, New York, 1979.
28. Orozco, J. M., and Webb, G., *Appl. Catal.* **6,** 67 (1983).
29. Szymanski, R., Charcosset, H., Gallezot, P., Massardier, J., and Tournayan, L., *J. Catal.* **97,** 366 (1986).
30. Phoung, T. T., Massardier, J., and Gallezot, P., *J. Catal.* **102,** 456 (1986).
31. Lau, C. L., and Snyder, R. G., *Spectrochim. Acta.* **27,** 2073 (1971).
32. Chou, P., and Vannice, M. A., *J. Catal.* **104,** 1 (1987).
33. Chen, A. A., Benesi, A. J., and Vannice, M. A., *J. Catal.* **119,** 14 (1989).
34. van Meerten, R. Z. C., de Graaf, T. F. M., and Coenen, J. W. E., *J. Catal.* **46,** 1 (1977).
35. Selwood, P. W., and Webb, G., *Appl. Catal.* **79,** 4637 (1957).
36. Aben, P. C., van der Eijk, H., and Oelderik, J. M., *Int. Congr. Catal. Proc. 5th 1973* **2,** 48 (1973).
37. Sinfelt, J. H., Hurwitz, H., and Shulman, R. A., *J. Phys. Chem.* **64,** 1559 (1960).
38. Derbventsev, Yu. I., Paal, Z., and Tetenyi, P., *J. Phys. Chem.* **80,** 51 (1972).
39. Tetenyi, P., and Paal, Z., *J. Phys. Chem.* **80,** 63 (1972).
40. Smith, H. A., and Meriwether, H. T., *J. Amer. Chem. Soc.* **71,** 413 (1949).
41. Gonzo, E. E., and Boudart, M., *J. Catal.* **52,** 461 (1978).
42. Gland, J. L., and Somorjai, G. A., *Surf. Sci.* **38,** 157 (1973).